**Real-Time Kadanoff-Baym Approach to Nuclear Response Functions**

H. S. Köhler [1]
*Physics Department, University of Arizona, Tucson, Arizona 85721,USA*
N. H. Kwong [2]
*College of Optical Sciences, University of Arizona, Tucson, Arizona 85721, USA*

arXiv:1601.05463v1 [nucl-th] 20 Jan 2016

**Abstract**

Linear density response functions are calculated for symmetric nuclear matter of normal density by time-evolving two-time Green's functions in real time. Of particular interest is the effect of correlations. The system is therefore initially time-evolved with a collision term calculated in a direct Born approximation as well as with full (RPA) ring-summation until fully correlated. An external time-dependent potential is then applied. The ensuing density fluctuations are recorded to calculate the density response. This method was previously used by Kwong and Bonitz for studying plasma oscillations in a correlated electron gas. The energy-weighted sum-rule for the response function is guaranteed by using conserving self-energy insertions as the method then generates the full vertex-functions. These can alternatively be calculated by solving a Bethe -Salpeter equation as done in some previous works. The (first order) mean field is derived from a momentum-dependent (non-local) interaction while $2^{nd}$ order self-energies are calculated using a particle-hole two-body effective (or 'residual') interaction given by a gaussian *local* potential.

We present numerical results for the response function $S(\omega, q_0)$ for $q_0 = 0.2, 0.4$ and $0.8\text{fm}^{-1}$. Comparison is made with the nucleons being un-correlated i.e. with only the first order mean field included, the 'HF+RPA' approximation.

We briefly discuss the relation of our work with the Landau quasi-particle theory as applied to nuclear systems by Sjöberg and followers using methods developped by Babu and Brown, with special emphasis on the 'induced' interaction.

# 1 Introduction

Response functions, the response of a many-body system to an external perturbation is instrumental in our understanding of the properties and interactions involved in the excitations of the system. In the study of nuclear systems these response functions are of particular interest when it comes to calculate the mean free path and absorpton of e.g. neutrinos in a neutron gas [1, 2], a subject of interest in astrophysical studies.[3, 4]

This report concerns the calculation of linear density response functions for symmetric nuclear matter. The excitations of the medium in response to an external perturbation is of course closely dependent on the interactions in the medium. Of particular interest here is the effect of correlations i.e. dressed propagators and collision-terms. It was shown by Baym and Kadanoff [5] that, if one wishes to construct the linear response function with dressed equilibrium Green's functions, appropriate vertex corrections to the polarization bubble are necessary to guarantee the preservation of the local continuity equation for the particle density and current in the excited system, which in turn implies the satisfaction of the energy-weighted sum-rule. This problem has traditionally involved solving a Bethe-Salpeter equation to calculate these vertex corrections. Such a calculation was done by Bozek for nuclear matter[6] and further applied in ref.[7] while Lykasov et al used the Landau transport equation with a collision term and vertex corrections.[8] Response functions have of course since long been the focus of intense studies related to the electron gas. Early works by Lundqvist and Hedin are noticeable leading to the often cited GW method. [9, 10] More recent works include those of Faleev and Stockman focussing on electrons in quantum wells.[11]

An alternative method, that does not require an explicit solution of the Bethe-Salpeter equations, is a real time solution of the Kadanoff Baym two-time equations equations using conserving approximations for the self-energies. This method guarantees that the energy weighted sum-rule (assuming an effective mass $m^*$) $\int_0^\infty \omega S(\omega, q_0) d\omega = \frac{q_0^2}{2m^*}$ is satisfied. It was first used by Kwong and Bonitz for the plasma oscillations in an electron gas [12] and later in ref.[13]. They presented a fully linearised formalism separating the Green's function into a spatially homogeneous part $G_{00}$ and a linear response part $G_{10}$. As made clear in ref. [14] there is no need to separately calculate vertex corrections when applying this formalism. The proper vertex corrections are

[1] e-mail: kohler@physics.arizona.edu
[2] e-mail:kwong@optics.arizona.edu

generated by the time-evolution of the Green's functions when subjected to the external disturbance. We use this method here to calculate density response functions in symmetric nuclear matter.

The relevant KB-equations, already presented in ref. [12] are shown in section 2. followed in sect 2.1 by an exposé and explanation of the interactions used at the separate level of approximations. When the system initially correlates with the total energy being conserved, the potential energy of interactions decreases and the kinetic energy increases, resulting in an increase of the temperature. Section 2.2 shows how to calculate the resulting temperature after equilibration. Our main computed results are shown in Sect. 3. The relation of of our work to the Landau quasi-particle theory is addressed in Sect. 4 and Sect. 5 contains a summary of our results and some conclusions. A diagrammatic representation of the main equations is shown in an Appendix.

# 2 The two-time KB-equations

The Kadanoff-Baym equations in the two-time form for the specific problem at hand was already shown in previous work, where it was applied to the electron gas in a linear response calculation.[12] Some modifications (related to the difference in interactions and self-energies) are necessary for the present nuclear problem. Correlations are included by defining self-energies in a second order Born approximation with a residual interaction defined by eq.(17) below. This is in addition to a first order mean (Hartree-Fock) field. This then is a 'conserving approximation' [5] a necessary requirement when applying the two-time formalism consistently. We compare our results with calculations where correlations are neglected with only the mean field included, the 'HF+RPA' approximation.

We consider three separate cases:
I. Uncorrelated, mean field only, RPA approximation.
II. Correlations included by self-energies in second order Born of a residual interaction, eq.(17) below.
III. Correlations modified by including not only second order diagrams but ring-diagrams to all orders (i.e. RPA) in the self-energies.
The selfenergy obtained with the second order Born approximation as well as RPA are 'conserving approximations' [5] a necessary requirement when applying the two-time formalism consistently.

Calculations proceed as follows: Equilibrium Green's functions are first constructed for an uncorrelated fermi distribution of specified density and temperature. These functions, $G_{00}$, are then time-evolved (for typically $10fm/c$) with the chosen mean field and correlations (I,II or III above) until stationary. An external field $U(\mathbf{q},t) = U_0(t)\delta_{\mathbf{q},\mathbf{q_0}}$ is then applied which generates particle-hole Green's functions $G^{>}_{<10}$ that propagate in time according to equations already shown in ref. [12] and for completeness repeated here (summation over $m = 0, 1$ and integration over $\bar{t}$ from $-\infty$ to $+\infty$ is implied).

$$\left(i\hbar\frac{\partial}{\partial t} - \epsilon_{\mathbf{k+q_0}}\right) G^{>}_{<10}(\mathbf{k}tt') = U_0(t)G^{>}_{<00}(\mathbf{k}tt') + \Sigma^{HF}_{1m}(\mathbf{k}t)G^{>}_{<m0}(\mathbf{k}tt') + \Sigma^{R}_{1m}(\mathbf{k}t\bar{t})G^{>}_{<m0}(\mathbf{k}\bar{t}t') + \Sigma^{>}_{<1m}(\mathbf{k}t\bar{t})G^{A}_{m0}(\mathbf{k}\bar{t}t') \quad (1)$$

and

$$\left(-i\hbar\frac{\partial}{\partial t'} - \epsilon_{\mathbf{k}}\right) G^{>}_{<10}(\mathbf{k}tt') = U_0(t')G^{>}_{<11}(\mathbf{k}tt') + G^{>}_{<1m}(\mathbf{k}tt')\Sigma^{HF}_{m0}(\mathbf{k}t') + G^{R}_{1m}(\mathbf{k}t\bar{t'})\Sigma^{>}_{<m0}(\mathbf{k}\bar{t}t') + G^{>}_{<1m}(\mathbf{k}t\bar{t'})\Sigma^{A}_{m0}(\mathbf{k}\bar{t}t') \quad (2)$$

We point out that $G^{>}_{<10}$ 'carries' two momenta; $G^{>}_{<10}(\mathbf{k}tt') \equiv G^{>}_{<10}(\mathbf{k}+\mathbf{q_0}, t; \mathbf{k}, t')$. [12]

In case III the rings are included in the selfenergies $\Sigma^{>}_{<00}$ by

$$\Sigma^{>}_{<00}(\mathbf{k},t,t') = i\sum_{\mathbf{p}} G^{>}_{<00}(\mathbf{k}-\mathbf{p},t,t')V^{>}_{s<}(\mathbf{p},t,t'). \quad (3)$$

with

$$V_s^{\gtrless}(\mathbf{p},t,t') = V(\mathbf{p})[\int_{t_0}^{t} dt''(\Pi_{00}^{>}(\mathbf{p},t,t'') - \Pi_{00}^{<}(\mathbf{p},t,t''))V_s^{\gtrless}(\mathbf{p},t'',t') - \int_{t_0}^{t'} dt''\Pi^{\gtrless}(\mathbf{p},t,t'')(V_s^{>}(\mathbf{p},t'',t') - V_s^{<}(\mathbf{p},t'',t'))] + V^2(\mathbf{p})\Pi_{00}^{\gtrless}(\mathbf{p},t,t') \quad (4)$$

where $V(\mathbf{p})$ is the momentum-representation of the residual potential, local in ccordinate space, eq. (17). The polarisation bubble $\Pi_{00}$ is defined by

$$\Pi_{00}^{\gtrless}(\mathbf{p},t,t') = -i\sum_{\mathbf{p}'} G_{00}^{\gtrless}(\mathbf{p}',t,t')G_{00}^{\lessgtr}(\mathbf{p}'-\mathbf{p},t',t) \quad (5)$$

In a second order calculation (case II) only the last term (one bubble) in eq. (4) will contribute to $V_s$.

The polarisation bubble in the (10)-channel is given by

$$\Pi_{10}^{\gtrless}(\mathbf{p},t,t') = -i\sum_{\mathbf{p}'}[G_{10}^{\gtrless}(\mathbf{p}',t,t')G_{00}^{\lessgtr}(\mathbf{p}'-\mathbf{p},t',t) + G_{00}^{\gtrless}(\mathbf{p}',t,t')G_{10}^{\lessgtr}(\mathbf{p}'-\mathbf{p}-\mathbf{q_0},t',t)] \quad (6)$$

and the selfenergies in the (10) channel are given by

$$\Sigma_{10}^{\gtrless}(\mathbf{k},t,t') = i\sum_{\mathbf{p}}[G_{10}^{\gtrless}(\mathbf{k}-\mathbf{p},t,t')V_s^{\gtrless}(\mathbf{p},t,t') + G_{00}^{\gtrless}(\mathbf{k}-\mathbf{p},t,t')V_{s(10)}^{\gtrless}(\mathbf{p},t,t')] \quad (7)$$

In case III where rings are included to all orders one has

$$V_{s(10)}^{\gtrless}(\mathbf{p},t,t') = a_{10}^2\int_{t_0}^{t} d\bar{t}\int_{t_0}^{t'} d\bar{t}' \{V_s^R(\mathbf{p}+\mathbf{q_0},t,\bar{t})\Pi_{10}^R(\mathbf{p},\bar{t},\bar{t}')V_s^{\gtrless}(\mathbf{p},\bar{t}',t') + V_s^R(\mathbf{p}+\mathbf{q_0},t,\bar{t})\Pi_{10}^{\gtrless}(\mathbf{p},\bar{t},\bar{t}')V_s^A(\mathbf{p},\bar{t}',t') + V_s^{\gtrless}(\mathbf{p}+\mathbf{q_0},t,\bar{t})\Pi_{10}^A(\mathbf{p},\bar{t},\bar{t}')V_s^A(\mathbf{p},\bar{t}',t')\} \quad (8)$$

See following section regarding the $a_{10}$-factor and interactions. The retarded and advanced parts are given by

$$\Sigma_{10}^{R/A}(\mathbf{p},t,t') = \pm\theta(\pm(t-t')[\Sigma_{10}^{>}(\mathbf{p},t,t') - \Sigma_{10}^{<}(\mathbf{p},t,t')] \quad (9)$$

$$\Pi_{10}^{R/A}(\mathbf{p},t,t') = \pm\theta(\pm(t-t')[\Pi_{10}^{>}(\mathbf{p},t,t') - \Pi_{10}^{<}(\mathbf{p},t,t')] \quad (10)$$

$$V_s^{R/A}(\mathbf{p},t,t') = \delta(t-t')V(\mathbf{p}) \pm \theta(\pm(t-t')[V_s^{>}(\mathbf{p},t,t') - V_s^{<}(\mathbf{p},t,t')] \quad (11)$$

In case II $V_{s(10)}$ simplifies to

$$V_{s(10)}^{\gtrless}(\mathbf{p},t,t') = V_a(\mathbf{p})V_a(\mathbf{p}+\mathbf{q_0})\Pi_{10}^{\gtrless}(\mathbf{p},t,t') \quad (12)$$

with $V_a$ specified below in section 2.1.

For the Hartree-Fock self-energy in the (00)-channel we choose a parametrisation shown in section 2.1 below. The Hartree-Fock self-energy in the (10)-channel is given by

$$\Sigma_{10}^{HF}(\mathbf{p},t) = -iV_a(q_0)\sum_{\mathbf{p}'} G_{10}^{<}(\mathbf{p}',t,t) + i\sum_{\mathbf{p}'} G_{10}^{<}(\mathbf{p}-\mathbf{p}',t,t)V_a(p') \tag{13}$$

A diagrammatic representation of the above equations is shown in the Appendix.

The eqs. (1) and (2) are time-evolved and the response-function is, after a fourier-transformation of

$$\delta n(q_0,t) = -i\sum_{\mathbf{p}} G_{10}^{<}(\mathbf{p},t,t)$$

with respect to time t, calculated from

$$S(\omega,q_0) = \frac{\delta n(q_0,\omega)}{\pi n_0 U_0(\omega)}\delta n(q_0,\omega) \tag{14}$$

## 2.1 Interactions

The nuclear two-body problem in 'free space' is still unresolved in detail but it involves a combination of long ranged one-pion exchange contributions and complicated strong short ranged interactions and repulsions. This leads to even more complicated 'in-medium' interactions and strong correlations in the nuclear many-body environment. Simplifications are necessary to make the exploratory calculations presented here reasonably short. The nuclear model adopted in most similar works is that of nucleons moving in a mean (' Hartree-Fock self-consistent') field with mutual in-medium ('residual') two-body interactions defined by some potential. A reasonable form of this potential could be a Skyrme- ( as used in ref. [15]) or the Gogny-interaction ( as used in ref. [16, 17]) or some similar interaction. Apart from these in-medium effective potentials, a semi-realistic NN-interaction with a hard core was used in a Jastrow-correlated extension of the RPA.[18]. We are taking a somewhat different approach here adopting three different potentials (A,B and C)' each representing different aspects (domains) of the interaction that for the purpose of presentation we assume to be a Brueckner state-independent reaction matrix $<\mathbf{k}|K|\mathbf{k}'>$ or $K(\mathbf{p},\mathbf{q})$ with $q = \mathbf{k}-\mathbf{k}'$ and $p = \frac{1}{2}(\mathbf{k}+\mathbf{k}')$.

A. An important feature of the Hartee-Fock mean field is that it is momentum-dependent and that only the diagonal matrix-elements $K(p,0)$ are needed for its calculation. We adopt a parametrisation due to Welke et al [19] leading to:

$$\Sigma_{00}^{HF}(\mathbf{p},t) = A\frac{\rho}{\rho_o} + B\left(\frac{\rho}{\rho_0}\right)^{\sigma} + 2\frac{C}{\rho_o}\int \frac{\rho(\mathbf{p}',t)}{1+(\frac{\mathbf{p}-\mathbf{p}'}{\Lambda})^2}\frac{d\mathbf{p}'}{(2\pi)^3} \tag{15}$$

with $A = -110.44$ MeV, $B = 140.9$ MeV, C=-64.95 MeV, $\sigma = 1.24$, $\rho_o = 0.16\text{fm}^{-3}$ , $\Lambda = 1.58p_F$ while $\rho$ is the density of the symmetric nuclear matter under consideration and $\rho(\mathbf{p},t)$ is defined below.

We shall also, in separate calculations substitute this mean field by assuming an effective mass.

B. To calculate the second order Born and ring diagrams we need off-diagonal matrix-elements of the interaction i.e. its $q$-dependence. We choose here an interaction often used in this context and first introduced by Danielewicz [6, 7, 20, 21] given by:

$$V(r) = V_0 e^{-(\frac{r}{\eta})^2} \tag{16}$$

with $\eta = 0.57$fm and $V_0 = -453$ MeV.

In momentum-space it reads:

$$V(\mathbf{q}) = \pi^{3/2}\eta^3 V_0 e^{-\frac{1}{4}\eta^2 q^2} \tag{17}$$

We use this interaction to calculate self-energies $\Sigma_{00}^{<}$ and $\Sigma_{00}^{>}$.

C. The linear response calculation involves excitations near the fermi-surface i.e. matrix-elements $K(q, p\sim p_F)$ for which the $p$-independent interaction (17) is too strong, leading to divergences if used for calculating the (10) field components. This is related to a too large numerical value of the related Landau parameter. Numerical results shown below are therefore made introducing a strength factor $a_{10}$ to define an interaction $V_a(q) = a_{10}V(q)$. The majority of the calculations presented below are with $a_{10} = 0.3$. Other values are chosen below together with a discussion of the Landau parameter. (See section 4)

### 2.2 Equilibrium Temperature

In a KB-calculation with selfenergies defined by a conserving approximation the total energy is conserved; while the potential energy decreases and kinetic energy increases with the same amount until internal equilibrium. The result is an increase in temperature from the initially set value. This situation can be moderated by an imaginary time-stepping method. [20, 21, 22] The final temperature $T_f$ in equilibrium will be a function of the initial imaginary time $\tau$ (and initial temperature) with $T_f \to 0$ in the limit $\tau \to \infty$.

The temperature $T_f = 1/\beta$ and chemical potential $\mu$ are then related to the equilibrium self-energies $\Sigma^<$ and $\Sigma^>$ by [23]:

$$\Sigma^>(\mathbf{p},\omega) = -e^{\beta(\omega-\mu)}\Sigma^<(\mathbf{p},\omega). \tag{18}$$

(The ratio of the selfenergies is consequently independent of momentum $\mathbf{p}$, which serves as a check on numerical accuracy.)

With $\beta$ and $\mu$ calculated from eq. (18) the equilibrium uncorrelated distribution function is given by

$$f(p) = 1/(1 + e^{\beta(\omega(p)-\mu)}) \tag{19}$$

with

$$\omega(p) = p^2/2m + Re\Sigma^+(\mathbf{p},\omega) + \Sigma_{00}^{HF}((\mathbf{p})) \tag{20}$$

The real part of $\Sigma^+$ is calculated from the imaginary part by the dispersion relation, and using the relation

$$2Im\Sigma(\mathbf{p},\omega) = i(\Sigma^<(\mathbf{p},\omega) - \Sigma^>(\mathbf{p},\omega) \tag{21}$$

While the uncorrelated distribution is given by eq. (19) the correlated one is given by

$$\rho(\mathbf{p},t) = -iG^<(\mathbf{p},t,t). \tag{22}$$

# 3 Numerical Results

Calculations are made for symmetric nuclear matter at normal nuclear matter density; $\rho = 0.13\text{fm}^{-3}$, i.e. fermi-momentum $k_F = 1.25\text{fm}^{-1}$. The external momentum transfer is chosen to be either $q_0 = 0.2, 0.4$ or $0.8\text{fm}^{-1}$. The calculations follow essentially the computing-methods described in ref. [24] with the additional requirement to also time-evolve $G_{10}$. The eq. 8 is solved as a matrix equation.

All numerical results shown below are without the initial imaginary time-stepping referred to above. The initial (t=t'=0) distribution $\rho(p) = -iG_{00}^<(p,0,0)$ is taken to be a zero temperature fermi-distribution except in the uncorrelated case where $T = 5$ MeV.(See below.) The system is then time-evolved and correlations are completed at $t \geq t_c$, with $t_c$ being the correlation time. In the linear response evolution used here, separating the Green's function into $G_{00}$ and $G_{10}$ components, the collision term for the $G_{00}(p,t,t)$ evolution will vanish for $t > t_c$ and the distribution $\rho(p)$ is then stationary. (See ref. [22] for a detailed discussion of correlation times $t_c$.)

Fig. 1 shows the relevant distribution-functions. Solid lines show the initial zero-temerature Fermi-distribution and two correlated distributions corresponding to the three cases I,II,and III. The temperatures calculated from eq. (18 are in cases II and III $T_f = 5.4$ and 5.5 MeV respectively, while in case I the temperature is $T_f = T_i = .0$. The broken curve shows the $T = 5$ MeV Fermi-distribution.

The result of the correlations is a depletion of occupation below the fermimomentum and scattering into states above this mommentum. It is very similar to results obtained with more 'realistic' interactions/citehsk92. We therefore claim that the correlations induced with our simple model-interaction are 'realistic'. With the correlations completed in the (00) channel the external field $U_0(t)$ is now applied generating the $G_{10}$ field as shown by eqs. (1) and (2). Note that with the conserving approximation satisfied the vertex-correction is 'automatically' included in the ensuing time-evolution.[12]

The resulting time dependent density

$$\delta n(q_0,t) = -i\sum_{\mathbf{p}} G_{10}^<(\mathbf{p},t,t)$$

is recorded until it is fully damped. If the damping time is too large (number of time-steps $>\sim 150$) then $n(q_0,t)$ is extrapolated using the amplitudes and frequencies of the oscillations for lesser times. A typical result of the evolution in real time is shown in Fig. 2. This time-function is then fourier-transformed to $\omega$-space. Results for the three different examples of self-energies referred to in the Introduction are shown below.

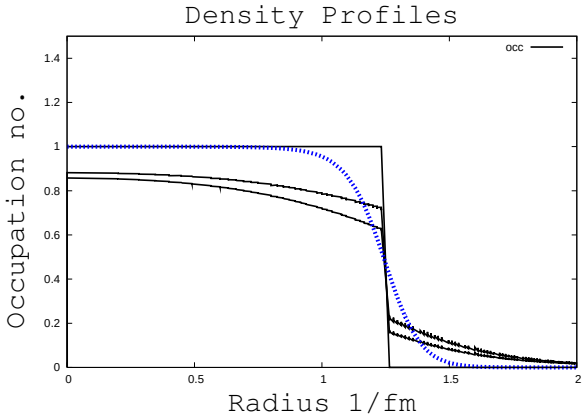


Figure 1: Solid lines show the zero temperature Fermi-distribution (top curve), the correlated distribution with the second-order selfenergy calculations (second from top) while the bottom curve is with RPA selfenergys. The broken curve (blue on-line) is a $T = 5$ MeV Fermi-distribution.

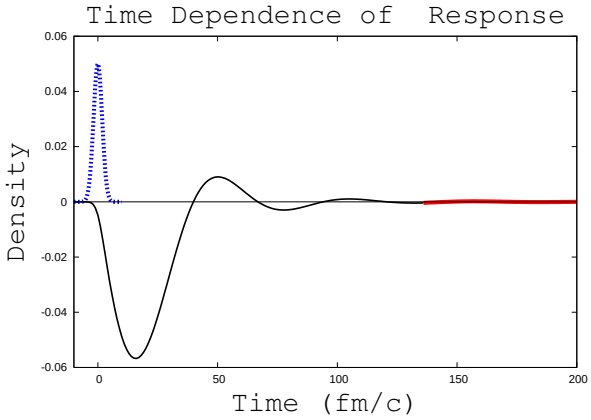


Figure 2: The solid curve shows the density $\delta n(q_0, t)$ with $q_0 = 0.4\text{fm}^{-1}$ for $t < 120 fm/c$ and extrapolated for $t > 120 fm/c$ (red on-line). The broken curve (blue on-line) shows the external field $U(q_0, t)$ with a maximum of 50 MeV at $t = 0$.

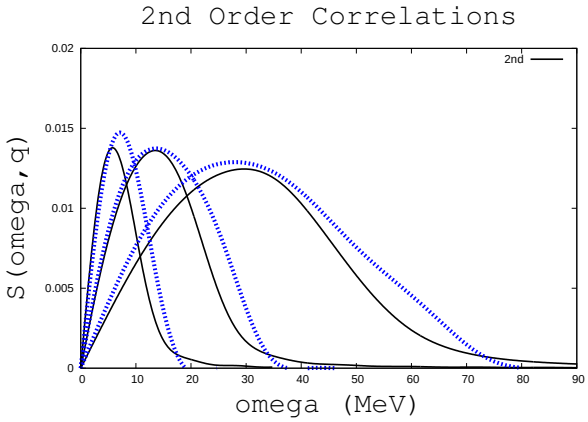


Figure 3: Solid curves show response functions $S(\omega, q_0)$ with $2^{nd}$ order correlations (case II) included. External momentum transfers are $q_0 = 0.2, 0.4$ and $0.8\text{fm}^{-1}$ respectively. They are compared with HF+RPA (case I) results at temperatures T=5 MeV: broken curves (blue online). See text for further explanations.

### 3.1 Mean field +RPA; case I

All selfenergies except the HF are here identically zero. Results of these calculations are shown by the broken lines (blue on-line) in Fig. 3. (For comparison with the correlated cases (II and III) the temperature is here chosen to be 5 MeV).

There is an overall agreement with previous RPA calculations e.g. [7, 15, 16]. There are some differences to be expected because of the variety of two-body interactions and mean fields that have been used. Our results here are displayed mostly for comparison with the results below where correlations beyond HF are considered. The heating to $T = 5$ MeV causes only a very slight broadening in comparison with a $T = 0$ calculation.

### 3.2 $2^{nd}$ order correlations; case II

The Green's functions are in this section dressed by second order insertions but no rings. This means that only the last term in eq. (4) is kept here i.e.:

$$V_s^{>}_{<}(\mathbf{p}, t, t') = V^2(\mathbf{p})\Pi^{>}_{00<}(\mathbf{p}, t, t')$$

and

$$V^{>}_{s(10)<}(\mathbf{p}, t, t') = V_a^2(\mathbf{p})\Pi^{>}_{10<}(\mathbf{p}, t, t')$$

The initial temperature at time $t = 0$ is here equal to zero; the momentum-distribution is that of a zero-temperature fermi-distribution. The correlations result in a heating to $T = 5$ MeV and an associated smoothing of the fermi-surface. An additional and more significant smoothing is due to the broadening of the static spectral-functions in the correlated medium, related to the imaginary parts of the self-energies also resulting in a considerable depletion of the distribution at low momenta.(See Fig. 1) This is the most probable cause for the difference between the correlated and uncorrelated cases in the region of the large values of frequencies $\omega$ as shown in Fig. 3. Other than that there is in fact no other major effect of the correlations.

### 3.3 Full Ring-correlations; case III

The results above, showing the effect of including correlations to second order in the chosen interaction is here extended by also including polarisation bubbles (rings) to all orders. The relevant additional terms are included in eqs. 4 and 8. This seems to be a logical extension of the second order calculation which just includes the lowest order of the full ring expansion. Rings to all orders are of course already generated in $G_{10}$ by the external disturbance $U(q_0, t)$, yielding the collective oscillations. Fig. 4 shows our result. The $2^{nd}$ order results included in Fig. 3 are for comparison also shown here by the broken (blue) lines. The effect is mainly that of some additional smoothing with a shift in the distribution from low to higher frequencies. This is related to the additional effect of correlations on the distribution functions shown in Fig. 1.

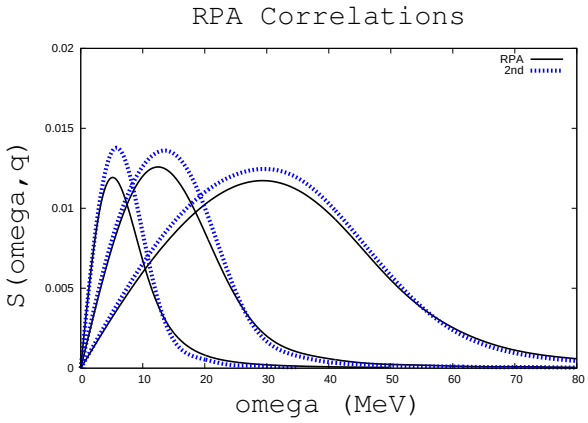


Figure 4: Solid curves show response functions $S(\omega, q_0)$ with full ring correlations (RPA) included and for external momentum transfers $q_0 = 0.2, 0.4$ and $0.8\text{fm}^{-1}$ respectively. They are compared with $2^{nd}$ order results: broken curves (blue online). See text for further explanations.

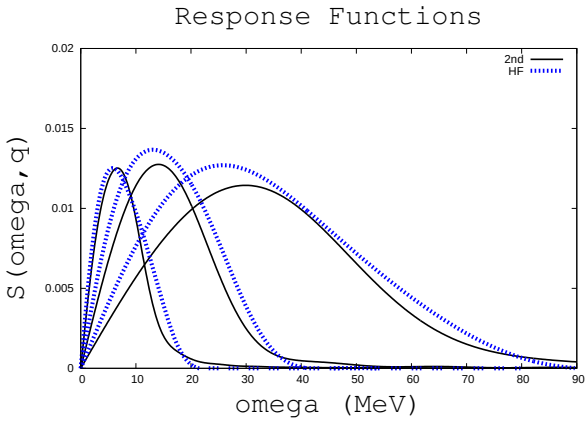


Figure 5: The second order (case II, solid lines) and the un-correlated case (case I, broken lines, blue on-line) response functions are shown here, both with the same mean field, defined by an effective mass $m^* = 0.7m$, implying $\Sigma_{00}^{HF}(p) \sim p^2$ .

### 3.4 Mean field and energy sum rule

Fig. 1 shows that the density-profiles $\rho(p)$ and therefore also the mean fields calculated from eq. (15) are different in each of the three cases that we considered. To see the effect this might have on our results shown so far we substituded the mean field $\Sigma_{00}^{HF}$ by an effective mass $m^* = 0.7$. The result is shown in Fig. 5. Compared with Fig. 3 one finds that the different mean fields have some effect but the differences at the high frequency tails of the response functions remain. This calculation also provides a test of the energy sum-rule,

$$\int_0^\infty \omega S(\omega, q_0) d\omega = \frac{q_0^2}{2m^*} \tag{23}$$

that cannot be directly validated with the mean field given by eq. (15) because it does not have a simple $p^2$ dependence. (The effective mass $m^*$ is $p$-dependent; $m^*(p) = \frac{p^2}{2m\Sigma^{HF}(p)+p^2}$.) With vertex corrections 'automatically' included in our 2-time formalism (see ref. [12]) this test is of no issue in the present work. It is in our calculations more a test of numerical consistency than a test of the formalism and this sum-rule was found to be satisfied within numerical accuracy.

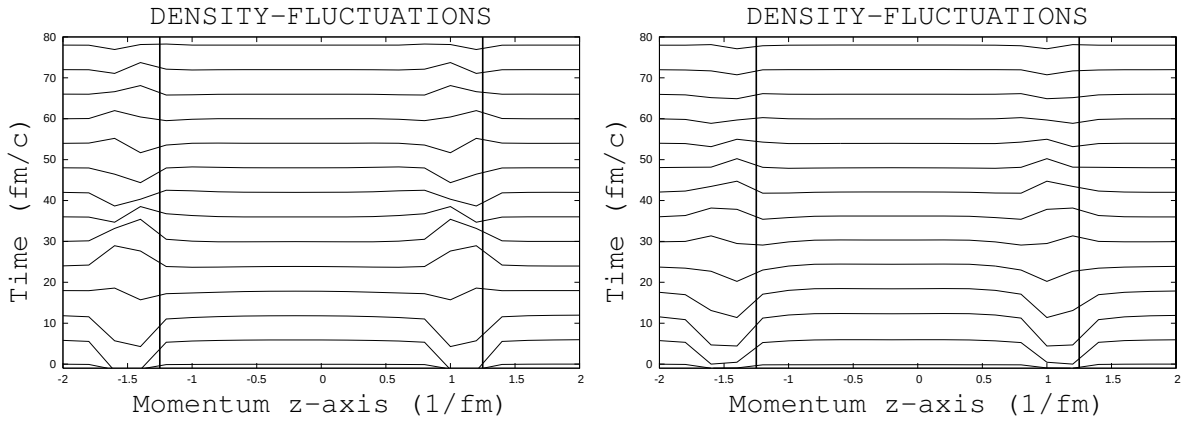


Figure 6: The perturbed density integrated over perpendicular momenta is shown as a function of momentum $p_z$ (with $\mathbf{q_0}$ along the z-axis) and time $t$; to the left with selfenergies are here calculated to second order and to the right . with selfenergies calculated to all orders of polarisation bubbles, i.e. RPA. The vertical lines (blue online) are at $p_z = \pm p_F$ (fermi-momentum).

### 3.5 Density Fluctuations

In order to show the approach to equilibrium in some detail the density $iG^<_{10}(\mathbf{p}, t, t)$ was integrated over $p_x$ and $p_y$ , ($p_z$ being the component along $\mathbf{q_0}$). The resulting $t$ and $p_z$ dependent functions are shown in Fig. 6 for $q_0 = 0.4\text{fm}^{-1}$ for selfenergies calculated to second (left figure) and all orders (right figure). One finds that the equilibration following the external perturbation is noticably faster when including the rings to all orders (full RPA) in the self-energies than to $2^{nd}$ order only.

This difference in damping between the two cases does not seem so obvious when comparing the corresponding response functions shown in Fig. 4, although a slight difference in the widths of the distributions can be noticed.

As already concluded above, the main effect of the correlations is to be found at the high frequency end of the response function. In the long wave-length limit the response function is mainly dependent on the excitations close to the fermi-surface shown by Fig. 6. The correlations result in states populated above the fermi-momentum that when excited by the external potential contribute to the energy spectrum at the high end of the response function.

# 4 Landau parameters

Owing to the relatively low temperature and long fluctuation wavelengths considered here, the excitations in our linear response calculations are concentrated around the fermi-surface. This is clearly evident from Fig. 6 which, as pointed out above, can explain why the effect of the correlations have a smaller effect than might be expected, repopulating the states close to the fermi-surface. This is also why Landau-theory would be applicable here as the quasi-particle picture dominates scatterings close to the fermi-surface. Another related reason why this theory is pertinent to our work is the relation [28] between the dimensionless Landau-parameter

$$F_0 = \frac{2m^* k_F}{\pi^2 \hbar^2} f_0 \tag{24}$$

and the summation of ring-diagram correlations, the collective excitation we are dealing with here. The factor $f_0$ is here the angular momentum ($l = 0$) quasi-particle (effective) interaction. This Landau parameter relates to the compressibility $K$ by

$$K = 6e_F(1 + F_0) \tag{25}$$

The interaction $f_0$ is composed of a 'direct' part defined by the functional derivative

$$f_{\mathbf{k}\mathbf{k}'} = \frac{\partial^2 E}{\partial n_{\mathbf{k}} n_{\mathbf{k}'}}$$

(with $\mathbf{k} \to \mathbf{k}'$) and an 'induced' part.

The 'induced' interaction relates to our discussion above as it is essentially the effect of screening by the ring-diagrams. It is defined below. Screening was first included in nuclear shell model calculations by Bertsch by a second order 'core-polarisation' diagram.[29] and later calculated to all orders by Kirson.[30]

Guided by methods used by Babu and Brown [28], who considered interactions in liquid $^3He$, Sjöberg [31] and later others (see e.g. ref. [32]) calculated Landau parameters for nuclear matter. They used Brueckner's $K$-matrix expression for the total energy $E$ in their analysis. The 'direct' interaction is then just the Brueckner $K$-matrix while the 'induced', $f_i$ is of higher orders of $K$. They find it to be given by

$$f_i(\mathbf{k}, \mathbf{k}) = -\sum_{\mathbf{p},\mathbf{p}'} f(\mathbf{k}, \mathbf{p}) \left( \frac{\delta n_{\mathbf{p}}(\mathbf{q}, \omega)}{\delta U_{\mathbf{p}'}(\mathbf{q}, \omega)} \right)_{q,0} f(\mathbf{p}'\mathbf{k})$$

Note that the perturbative potential $U_(\mathbf{p}')$ is here assumed to act on particles of momenta $\mathbf{p}'$ only, to generate density fluctuation $\delta n_{\mathbf{p}}$. Our interactions are not 'realistic' enough to warrant a detailed comparison with Sjöberg's (or other's based on Brueckner theory). It is here made only to illustrate the connection of our work with that based on Brueckner theory.[28, 31] For an approximate comparison we calculate the 'induced' interaction by

$$f_i = V_a^2(0) \frac{\delta n_{max}}{U_{max}}$$

,where as shown in Fig. 2 $U_{max} = 50$ MeV and $\delta n_{max}$ is the maximum in the density fluctuation. From the result of the calculation of response function shown in Fig. 3 (2nd order correlations) for $a_{10} = .3$ and for $q = 0.2\text{fm}^{-1}$ we find $\frac{\delta n}{\delta U} = .00126$ to get for the 'induced' interaction 24 Mevfm$^3$ with the 'direct' being $-140$ MeV fm$^3$ to get $F_0 = -0.495$. For comparison Sjöberg obtained $F_0 = -0.373$ for the angular momentum l=0 state. When comparing the two results one has to remember that Landau theory is a quasi-particle theory while our calculation goes beyond the quasi-particle with complex self-enrgies and non-zero spectral widths. Also, our result is with $q_0 = 0.2\text{fm}^{-1}$ not $q_0 = 0$ which is not dirctly attainable with our method.

The comparison of our calculated value of $F_0$ with that of Sjöberg's suggests however that our choice $a_{10} = 0.3$ is somewhat too large. Table 1 shows the dependence of $F_0$ on the strength parameter $a_{10}$ and Fig. 7 shows the response function $S(\omega, q_0 = 0.4\text{fm}^{-1})$ for $a_{10} = .1, .2, .3$ and 0.4.

The result is as to be expected; a considerable shift of the distribution with the strength. The stronger interaction excites states deeper in the fermi-sea while the weaker only excites states at the edge of the distribution i.e. of higher energy.

We showed how the Landau parameters can be calculated from our response function calculations. Alternatively, the response-function may be calculated using interactions given by Landau parameters. There are several published results using this method. (see ref. [33] and references therein).

TABLE

| | $a_{10}$ | $f_0^{(d)}$ | $f_0^{(i)}$ | $F_0$ |
|---|---|---|---|---|
| | 0.1 | -47.0 | 2.0 | -0.190 |
| | 0.2 | -93.0 | 10.0 | -0.356 |
| | 0.3 | -140.0 | 24.0 | -0.495 |
| | 0.4 | -187.0 | 46.0 | - 0.602 |

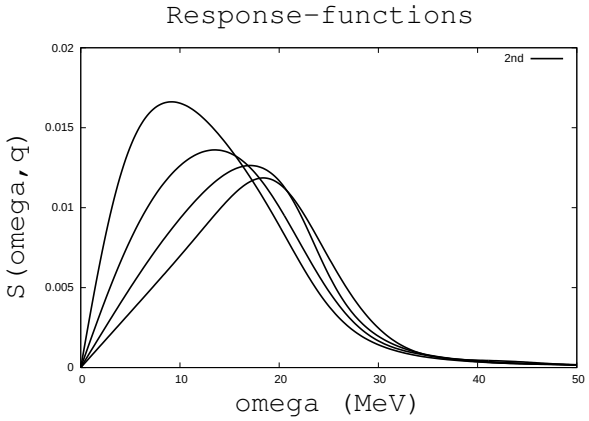


Figure 7: Solid curves show response functions $S(\omega, q_0 = 0.4)$ with second order self-energies and for $a_{10} = 0.4, 0.3, 0.2$ and 0.1 respectively from left to right. An effective mass $m^* = 0.7$ was used here.

# 5 Summary and Conclusions

The main purpose of this presentation is to illustrate the usefulness of the two-time Green's function (Kadanoff-Baym) method for the study of nuclear response. It was previously applied to the electron gas to see the effect of correlations.[12] The time-evolution of Green's function in two-time space with conserving approximations for the self-energies guarantees the preservation of the energy sum-rule. Alternative methods (in $\omega$-space) has been reported by Bozek et al.[6, 7] and by Lykasov et al.[8].

It may be a matter of choice but it seems that the two-time method has some advantages numerically. Calculations at zero temperature and/or with small values of $q_0$ for which the spectral width is small, are for instance a problem when working in $\omega$-space, but less so in the 2-time calculation.

The rise in temperature associated with the onset of correlations when using the two-time method is sometimes cited as a drawback. It is however not difficult to remedy by allowing the correlations to initially form by propagating along the imaginary time-axis. This was not done here but left for future works.

Comparing the various results obtained so far in our on-going investigation one finds some differences between the three different approximations (collisionless, $2^{nd}$-order and full rings) at high frequencies with corresponding decreases (but without any significant shift) in peak energies. In this regard our result agrees with those of ref. [7]. Whether the effect of correlations on e.g. neutrino-absorption or other medium sensitive reactions is important or not remains to be investigated.

The method of the two-time Green's function time-evolution is well documented, but several improvements in its application to the problem of response remain, mainly problems associated with any nuclear many body calculation i.e. that of the NN-force itself as well as in-medium effects.

We here circumvented this problem by defining three different potential-strengths, $V_G(p), V(q)$ and $V_a(q)$ relating to the mean field, correlations and external field excitations respectively. This involved admittedly a rather *ad hoc* choice but acceptable for this preliminary investigation. The most important choice of these is that of $V_a(q_0)$ entering in the calculation of the Hartree field that is the driving mechanism of the response. The bulk of the numerical results shown above were all made with the parameter $a_{10} = 0.3$ defining the strength of $V_a$. The choice of this particular value for this strength-factor was not based on any 'state of the art' calculation of the in-medium effective interaction. It was only chosen as to provide a reasonable representation of the interactions at the fermi-surface It led to a reasonable value of the related Landau-parameter. We also showed the dependence of this parameter on the strength-factor $a_{10}$ as well as the corresponding response functionsi as

shown in Fig. 7.

Spin,isospin, tensor,spin-orbit and pairing are however also aspects of the interaction that are of interest to consider[7, 8, 26, 27, 33, 34, 35] but still remain to be included in our calculations where we only considered density fluctuations. It has in addition been shown that the non-central parts of the effective interactions are modified close to the fermi-surface.[36] This may in particular effect spin-excitations in the long-wave length limit with excitations close to the fermi-momentum.

Although our understanding of nuclear forces and of the nuclear many-body problem is under constant development it is still incomplete. There is however important present-day knowledge that can and should be incorporated to improve our nuclear response calculations.

One reason for choosing a local potential (eq. 16) as done here is simply that the 2-time computer-code ([24]) used here is restricted to this choice. Separable interactions have however been obtained from inverse scattering. They are 'realistic' in the sense that they by construction fit scattering and deuteron data. [37] They can now be incorporated in our calculations by a new 2-time code ([38]) developped specifically for these separable (non-local) potentials.

The results shown are for symmetric nuclear matter. Response calculations for neutron matter is of particular interest related to astrophysical problems, in particular neutrino-absorption.

As a further comment we like to point out that the self-energy insertions have been separated into a Hartree-Fock (mean field) that is real and a 'correlation' part which is complex. This can be done consistently in the case of weak interactions. With medium-dependent effective interactions such a separation is not well defined and can lead to double-counting. The real term of the 'correlation' part adds to the mean field but if derived from an effective interaction it would already be included in the mean field *if this mean field is derived from the same effective interaction.* So one may claim that a double-counting can occurr. We avoided this situation here by choosing the three different forms of interaction referred to above.

# 6 Appendix:Diagrammatic representation of linear response in the real-time non-equilibrium Green's function formalism

In this appendix, we summarize the linear response of the many-nucleon system to an external field in the real-time Green's function formalism [39, 40, 41, 42, 23, 43, 44]. We use the standard diagrammatic perturbation formulation of Green's functions on a double-time contour . The diagrammatic representation facilitates comparison with the equivalent finite-temperature equilibrium Green's function treatment when the zeroth-order (in the external field) many-body state is an equilibrium state. We note that the linear response theory as formulated here is more general than that based on equilibrium Green's functions. Our method of solution is valid when the zeroth-order state is itself evolving in time. Baym-Kadanoff's papers. The Green's functions are defined with time arguments residing on a double-time contour shown in Fig. 8. The single-nucleon basis orbitals are labeled by momentum $\mathbf{k}$, spin projection $\sigma = \pm\frac{1}{2}$, and isospin projection $\tau = \pm\frac{1}{2}$. The single-nucleon Green's function is defined as

$$G\left(\mathbf{k}_1\sigma_1\tau_1\bar{t}_1, \mathbf{k}_2\sigma_2\tau_2\bar{t}_2\right) = -i\langle T_C[a_{\mathbf{k}_1\sigma_1\tau_1}(\bar{t}_1)a^\dagger_{\mathbf{k}_2\sigma_2\tau_2}(\bar{t}_2)]\rangle \tag{26}$$

where $a_{\mathbf{k}\sigma\tau}(\bar{t})$ and $a^\dagger_{\mathbf{k}\sigma\tau}(\bar{t})$ respectively annihilates and creates a nucleon in state $(\mathbf{k}\sigma\tau)$ at time $\bar{t}$. In this paper, a bar over a time symbol indicates that the represented time resides on the double-time contour, denoted by $C$, in Fig. 8 while an unbarred time symbol represents a point on the regular time axis. $T_C$ represents time-ordering along the time contour $C$, and $\langle\cdots\rangle$ denotes taking an expectation value in the initial state of the system. The time $\bar{t}$ on $C$ can also be written as $(t, b)$ where $t$ is the regular time and $b = +(-)$ labels the branch $C_+$ ( $C_-$ ) that $\bar{t}$ is on. The Green's function can then be written in a four-component form $G^{b_1 b_2}\left(\mathbf{k}_1\sigma_1\tau_1 t_1, \mathbf{k}_2\sigma_2\tau_2 t_2\right)$

where

$$
\begin{aligned}
G^{+-}\left(\mathbf{k}_1\sigma_1\tau_1 t_1, \mathbf{k}_2\sigma_2\tau_2 t_2\right) &= i\langle[a^\dagger_{\mathbf{k}_2\sigma_2\tau_2}(t_2)a_{\mathbf{k}_1\sigma_1\tau_1}(t_1)]\rangle \qquad (27)\\
&\equiv G^{<}\left(\mathbf{k}_1\sigma_1\tau_1 t_1, \mathbf{k}_2\sigma_2\tau_2 t_2\right)\\
G^{-+}\left(\mathbf{k}_1\sigma_1\tau_1 t_1, \mathbf{k}_2\sigma_2\tau_2 t_2\right) &= -i\langle[a_{\mathbf{k}_1\sigma_1\tau_1}(t_1)a^\dagger_{\mathbf{k}_2\sigma_2\tau_2}(t_2)]\rangle \qquad (28)\\
&\equiv G^{>}\left(\mathbf{k}_1\sigma_1\tau_1 t_1, \mathbf{k}_2\sigma_2\tau_2 t_2\right)\\
G^{++}\left(\mathbf{k}_1\sigma_1\tau_1 t_1, \mathbf{k}_2\sigma_2\tau_2 t_2\right) &= -i\langle T_+[a_{\mathbf{k}_1\sigma_1\tau_1}(t_1)a^\dagger_{\mathbf{k}_2\sigma_2\tau_2}(t_2)]\rangle \qquad (29)\\
&= \theta(t_1-t_2)G^{>}\left(\mathbf{k}_1\sigma_1\tau_1 t_1, \mathbf{k}_2\sigma_2\tau_2 t_2\right) +\\
&\quad \theta(t_2-t_1)G^{<}\left(\mathbf{k}_1\sigma_1\tau_1 t_1, \mathbf{k}_2\sigma_2\tau_2 t_2\right)\\
G^{--}\left(\mathbf{k}_1\sigma_1\tau_1 t_1, \mathbf{k}_2\sigma_2\tau_2 t_2\right) &= -i\langle T_-[a_{\mathbf{k}_1\sigma_1\tau_1}(t_1)a^\dagger_{\mathbf{k}_2\sigma_2\tau_2}(t_2)]\rangle \qquad (30)\\
&= \theta(t_1-t_2)G^{<}\left(\mathbf{k}_1\sigma_1\tau_1 t_1, \mathbf{k}_2\sigma_2\tau_2 t_2\right) +\\
&\quad \theta(t_2-t_1)G^{>}\left(\mathbf{k}_1\sigma_1\tau_1 t_1, \mathbf{k}_2\sigma_2\tau_2 t_2\right)
\end{aligned}
$$

from which one can see that only two of the four components are independent. In Eqs. (29) and (30), $T_+$ denotes time-ordering and $T_-$ anti-time ordering (ordering operators with earlier ones on the left of later ones). The

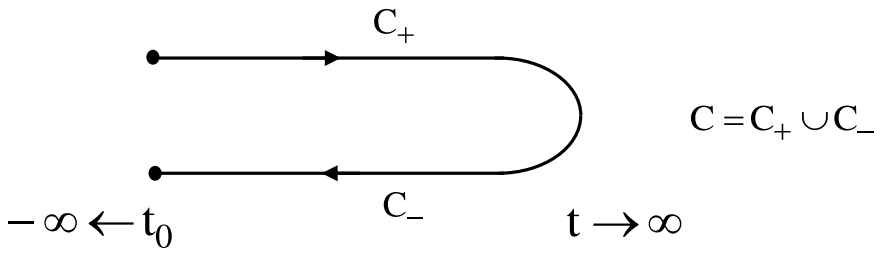


Figure 8: The double-time contour on which the non-equilibrium Green's functions are defined. The branch $C_+$ goes from a reference time $t_0$ in the distant past to $t \to \infty$, and $C_-$ goes from $\infty$ back to $t_0$.

perturbation theory for calculating the Green's functions and the diagrammatic tools that help implementing the theory can be found in e.g. [39, 40, 41, 42]. Grouping classes of diagrams yields equations of motion and non-perturbative approximation schemes for the Green's functions [23, 43, 44]. We show the diagrammatic content of the approximations we use for the linear response calculations in this paper. Fig. 9 shows the diagrams representing the equation of motion, or Dyson equation, of $G\left(\mathbf{k}_1\sigma_1\tau_1 t_1, \mathbf{k}_1\sigma_1\tau_1 t_2\right)$. The three parts show, (a) the full equation, (b) the equation to zeroth order in the external potential $U$, and (c) the equation to first order in $U$. The first order equation is written in terms of $G^{>}_{10}$ as Eqs. (1) and (2) in the main text, where the spin and isospin labels are omitted in the Green's functions. The self energies, to zeroth and first orders in $U$, are evaluated in this paper in various approximations, which are represented in Figs. 10 and 11. The diagrams representing processes up to the second Born approximation are shown in Fig. 10. In each equation in this figure, the first two diagrams on the right h and side give the Hartree-Fock approximation. The processes in the ring-diagram approximation are shown in Fig. 11, where the wavy line denotes the in-medium nucleon-nucleon interaction dressed by ring diagrams and is given in Fig. 12.

In the conventional formulation of linear (density) response theory (e.g. [45]), a retarded density correlation function, made up of equilibrium single-particle Green's functions, is calculated. For our nuclear matter system driven by the perturbation $(1/V)U(t)\sum\limits_{\mathbf{k}\sigma\tau} a^\dagger_{\mathbf{k}+\mathbf{q}\sigma\tau}a_{\mathbf{k}\sigma\tau}$ ($V$ being the normalization volume), the first-order density response carrying momentum $\mathbf{q}$, $\delta n(\mathbf{q},t) = \sum\limits_{\mathbf{k}\sigma\tau}\langle a^\dagger_{\mathbf{k}-\mathbf{q}\sigma\tau}(t)a_{\mathbf{k}\sigma\tau}(t)\rangle$, is written as

$$\delta n(\mathbf{q},t) = \frac{1}{\hbar}\int_{-\infty}^{\infty}\Pi^R(\mathbf{q},t-t')U(t') \qquad (31)$$

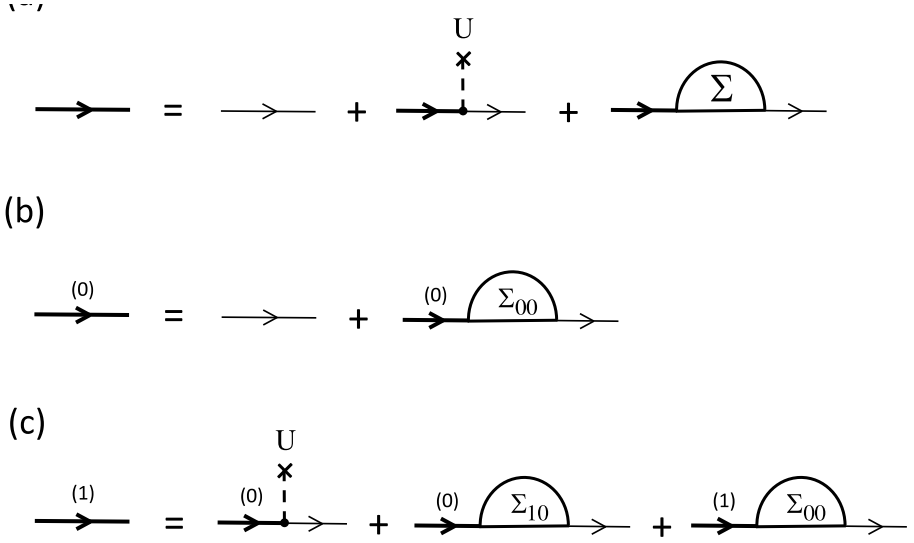


Figure 9: Dyson equation for the nonequilibrium single-nucleon Green's function. The thick solid directed line, the thin directed line, the dashed line labeled $U$, and the semicircle labeled $\Sigma$ denote, respectively, the Green's function, the free-nucleon Green's function, the external potential, and the self-energy. The number in parentheses, (0) or (1), above a Green's function line gives the order of $U$ in that Green's function. $\Sigma_{00}$ ($\Sigma_{10}$) is that part of $\Sigma$ evaluated to zeroth (first) order in $U$.

where the retarded density correlation $\Pi^R(\mathbf{q}, t-t')$ is defined as

$$\Pi^R(\mathbf{q}, t-t') = -\frac{i}{V}\theta(t-t')\sum_{\substack{\mathbf{k}\mathbf{k}'\\ \sigma\tau}}\langle[a^\dagger_{\mathbf{k}-\mathbf{q}\sigma\tau}(t)a_{\mathbf{k}\sigma\tau}(t), a^\dagger_{\mathbf{k}'+\mathbf{q}\sigma\tau}(t')a_{\mathbf{k}'\sigma\tau}(t')]\rangle_0 \tag{32}$$

where the subscript 0 indicates that the expectation value is taken in the equilibrium (unperturbed by $U(t)$) state. To calculate $\Pi^R(\mathbf{q}, t-t')$, it is related to the equilibrium Keldysh-time-ordered correlation function

$$\Pi(\mathbf{q}, \bar{t}, \bar{t}') = -\frac{i}{V}\sum_{\substack{\mathbf{k}\mathbf{k}'\\ \sigma\tau}}\langle T_C[a^\dagger_{\mathbf{k}-\mathbf{q}\sigma\tau}(\bar{t})a_{\mathbf{k}\sigma\tau}(\bar{t})a^\dagger_{\mathbf{k}'+\mathbf{q}\sigma\tau}(\bar{t}')a_{\mathbf{k}'\sigma\tau}(\bar{t}')]\rangle_0 \tag{33}$$

which may be evaluated in diagrammatic perturbation theory. Figs. 13 and 14 show the diagrams representing $\Pi(\mathbf{q}, \bar{t}, \bar{t}')$ that correspond to the three approximations to the perturbed self energy used in this paper. Our diagrammatic derivation of $\Pi(\mathbf{q}, \bar{t}, \bar{t}')$ is similar to that in [5]. We note again that all the single-nucleon Green's functions in these two figures are evaluated in the equilibrium state. Neglecting the quantity $L$ (represented by the rectangle labeled by $L$ in Fig. 13) would yield the random phase approximation. Containing the effects of exchange, correlations and collisions, $L$ is written as the solution of a Bethe-Salpeter equation (third equation in Fig. 13) driven by a vertex $K$. Each approximation for the perturbed self energy $\Sigma_{10}$ in our formulation corresponds to an equivalent selection of diagram set for $K$. These diagrams are drawn in Fig. 14. For each choice of diagrams for $K$, the single-nucleon Green's functions in the diagrams are dressed by the equilibrium self energy $\Sigma_{00}$ evaluated to the same level of approximation (Hartree-Fock, second Born, and ring diagrams) as that for the chosen $\Sigma_{10}$.

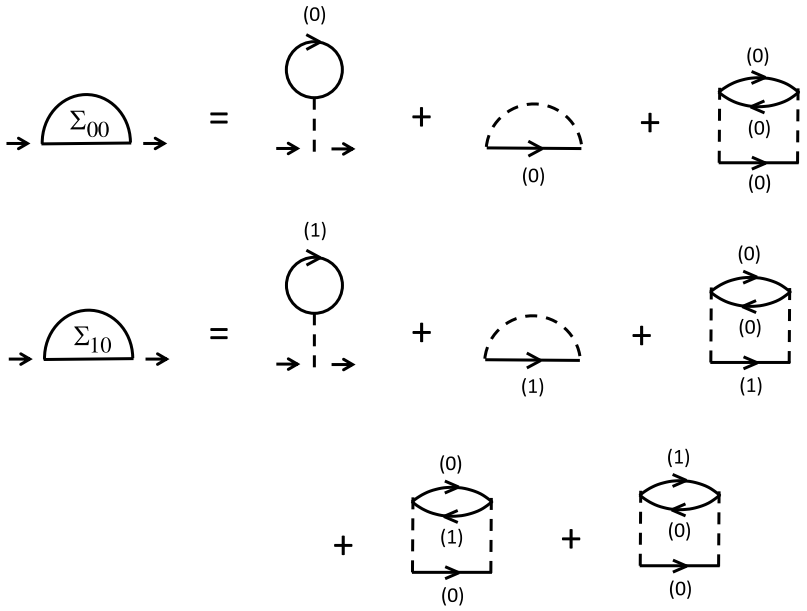


Figure 10: Zeroth and first order (in $U$) self energy in second order Born approximation. All solid lines are interacting Green's functions, and the dashed line denotes the nucleon-nucleon intera ction. In each equation, retaining only the first two terms yields the Hartree-Fock approximation.

# 7 Acknowledgements

One of us (HSK) wishes to thank The University of Arizona and in particular the Department of Physics for providing office space and access to computer facilities. This work has not been supported by any external agency.

# References

[1] J. Margueron, J. Navarro, P. Blottiau, Phys. Rev.C **70** 028801 (2004).

[2] Naoki Iwamoto and C.J. Pethick, Phys. Rev.D **25** 313 (1982).

[3] S. Reddy, M. Prakash, J. Lattimer, J. Pons Phys. Rev.C **59** 2888 (1998).

[4] A. Sedrakian and A. Dieperink, Phys. Rev.D **62** 083002 (2000).

[5] Gordon Baym and Leo P. Kadanoff, Phys. Rev. **124** 287 (1961) ; Gordon Baym, Phys. Rev. **127** 1391 (1962).

[6] P. Bozek, Phys. Letters **B579** 309 (2004).

[7] P. Bozek,J. Margueron and H. Müther, Ann. Phys.(N.Y.) **318** 245 (2005).

[8] G.I. Lykasov, E. Olsson and C.J. Pethick, Phys. Rev.C **72** 025805 (2005).

[9] L. Hedin , Phys. Rev. **139** A796 (1965).

[10] L. Hedin and S. Lundqvist, Solid State Physics (Acadenmic, New York, 1969) Vol 23.

[11] Sergey V. Faleev and Mark.I. Stockman Phys. Rev.B **63** 193302 (2001), Phys. Rev.B **66** 085318 (2002).

[12] N. H. Kwong and M. Bonitz, Phys. Rev. Letters **84** 1768 (2000).

[13] M. Bonitz, V. Golubnichiy, N. H. Kwong, D. Semkat, D. Kremp, V. S. Filinov and M. Schlanges, Contrib. Plasma Phys. **41** 155 (2001).

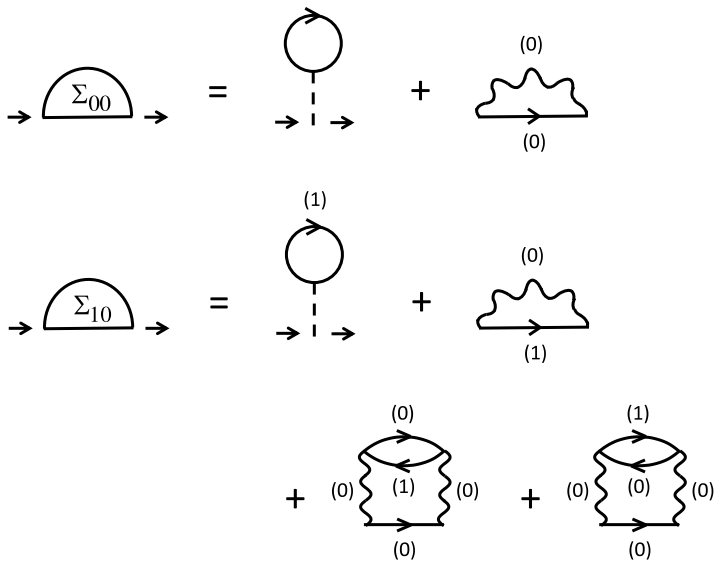


Figure 11: Self energy in the ring-diagram approximation. The wavy line denotes the nucleon-nucleon interaction dressed by ring diagrams which is shown in Fig. 12.

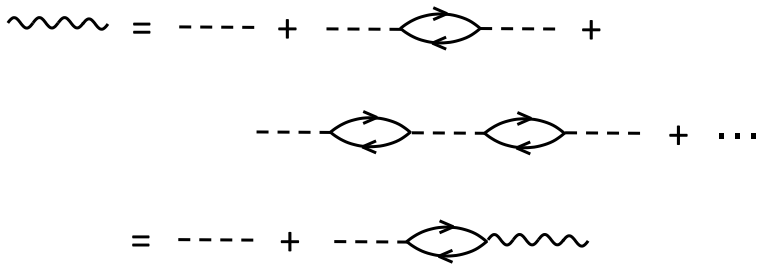


Figure 12: Nucleon-nucleon interaction dressed by ring diagrams. Note that the solid lines are fully dressed Green's functions.

[14] M. Bonitz, N. H. Kwong, D. Semkat and D. Kremp, Contrib. Plasma Phys. **39** 37 (1999)

[15] C. Garcia-Recio, J. Navarro,Van Gai Nguyen and L.L. Salcedo, Ann. Phys.(N.Y.) **214** 340 (1992).

[16] D. Gogny and R. Padjen, Nucl. Phys. A **293** 365(1977)

[17] J. Margueron, Nguyen Van Giai and J. Navarro, Phys. Rev.C **72** 034311 (2005).

[18] N H Kwong and D G Sandler, Phys. Lett. B **136** 1 (1984).

[19] G.M. Welke,M. Prakash, T.T.S. Kuos and S. Das Gupta, Phys. Rev.C **38** 2101 (1988).

[20] P. Danielewicz, Ann. Phys.(N.Y.) **152** 305 (1984).

[21] H.S. Köhler, Phys. Rev.C **51** 3232 (1995).

[22] H.S. Köhler and K. Morawetz, Phys. Rev.C **64** 024613 (2001).

[23] L. P. Kadanoff and G. Baym, *Quantum statistics mechanics* (W. A. Benjamin,New York, 1962).

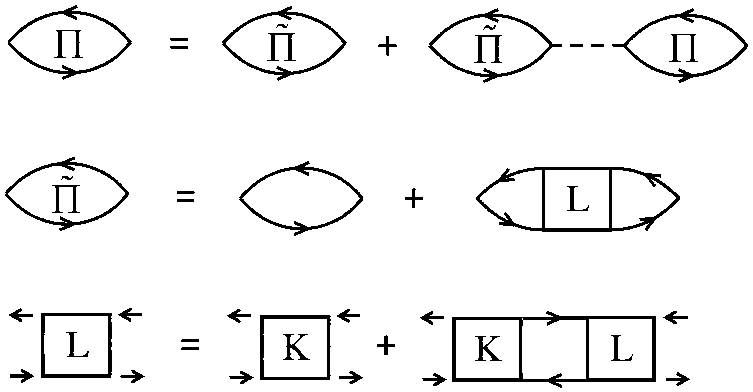


Figure 13: Diagrams representing the density correlation $i\Pi(\mathbf{q}, \bar{t}, \bar{t}')$ which yields the retarded correlation function in the conventional formulation of linear response. All solid lines in this figure and Fig. 14 represent equilibrium Green's functions (unperturbed by the external field $U$). The vertex $K$ for the approximations considered here is displayed in Fig. 14.


[24] H.S. Köhler, N.H. Kwong and Hashim A. Yousif, Comp.Phys.Comm. **123** 123 (1999)

[25] H.S. Köhler Nucl. Phys. A **537** 64 (1992)

[26] J. Dabrowski and P. Haensel , Ann. Phys.(N.Y.) **97** 452 (1976).

[27] E. Olsson, P. Haensel and C.J. Pethick, Phys. Rev.C **70** 025804 (2004).

[28] S. Babu and G.E. Brown, Ann. Phys.(N.Y.) **78** 1 (1973).

[29] G. F. Bertsch, Nucl. Phys. A **74** 234 (1965)

[30] Michael W. Kirson, Ann. Phys.(N.Y.) **66** 624 (1971).

[31] O. Sjöberg. Ann. Phys.(N.Y.) **78** 39 (1973).

[32] D. Gambacurta, U. Lombardo and w. Zuo, Physics of Atomic Nuclei, **74** 1424 (2011).

[33] A. Pastore, M. Martini, D. Davesne, K.Bennaceur, and J. Meyer, Phys. Rev.C **86** 044308 (2012); A. Pastore, D. Davesne and J. Navarro, J. Phys. G **41** 055103 (2014)

[34] J. Margueron, N. Van Giai and J. Navarro, Phys. Rev.C **74** 015805 (2006).

[35] Armen Sedrakian and Jochen Keller, nucl-th/1001.0395 Jochen Keller and Armen Sedrakian nucl-th/1205.6902

[36] Achim Schwenk and Bengt Friman, Phys. Rev. Letters **92** 082501 (2004).

[37] N.H. Kwong and H.S. Köhler, Phys. Rev.C **55** 1650 (1997).

[38] H.S. Köhler , to be published.

[39] L. V. Keldysh, Sov. Phys. JETP **20**, 1018 (1965).

[40] S. Fujita, J. Math. Phys. **6**, 1877 (1965).

[41] R. A. Craig, J. Math. Phys. **9**, 605 (1968).

[42] P. Danielewicz, Ann. of Physics **152**, 239 (1984).

[43] W. Botermans and R. Malfliet, Phys. Rep. **198**, 115 (1990).

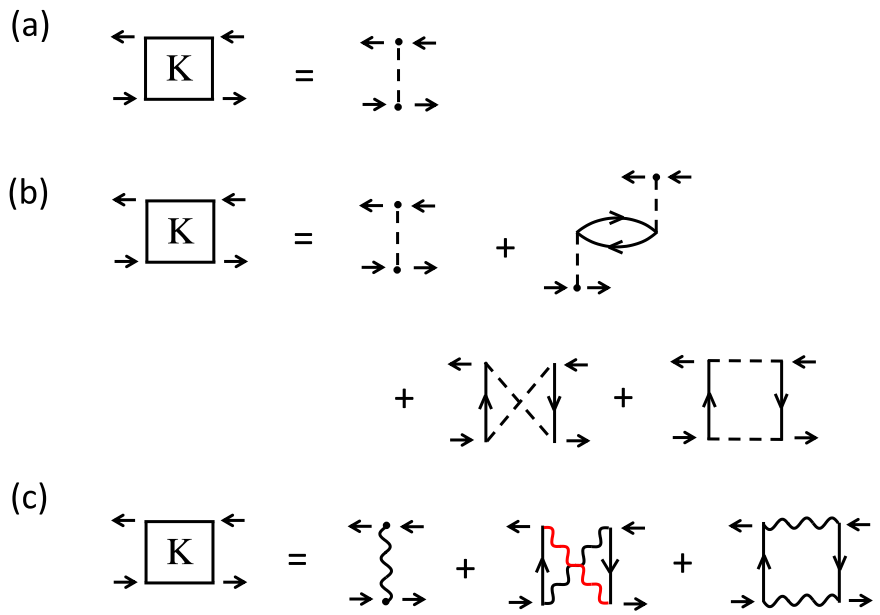


Figure 14: The diagrams representing the vertex $K$ in Fig. 13 that are equivalent to the three self-energy approximations used in this paper: (a) Hartree-Fock, (b) second Born, and (c) ring diagrams. One interaction line in (c) is drawn in red to help make the diagram clearer.

[44] D. Kremp, M. Schlanges, W.-D. Kraeft, and T. Bornath, *Quantum statistics of nonideal plasmas* (Springer, Berlin, 2005).

[45] A. L. Fetter and J. D. Walecka, *Quantum theory of may-particle systems* (McGraw-Hill, New York, 1971).

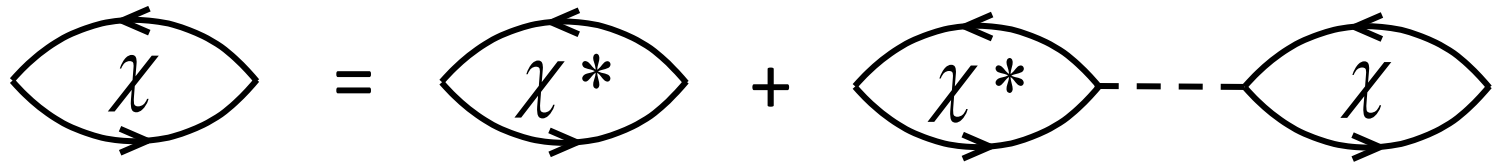
χ
=
χ*
+
χ*
χ

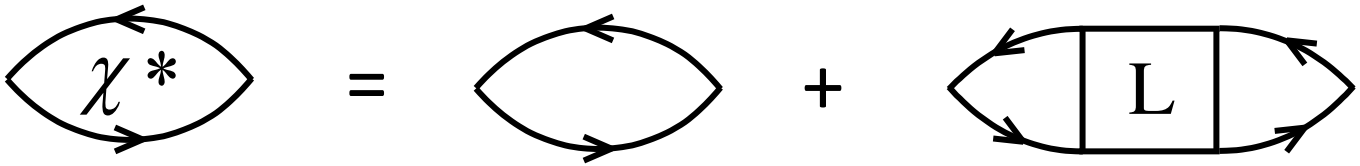
χ*
=
+
L

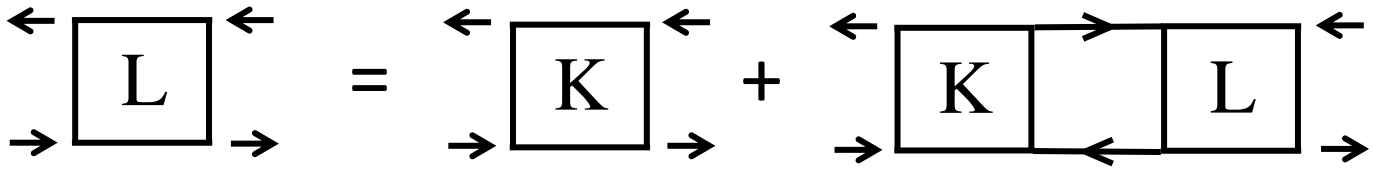
L
=
K
+
K
L